Supporting information

Differential Flap Dynamics in L,D-Transpeptidase2 from Mycobacterium Tuberculosis Revealed by Molecular Dynamics

Zeynab Fakhar,[a] Thavendran Govender,[a] Glenn E. M. Maguire,[a,b] Gyanu Lamichhane,[c] Ross C. Walker,[d,e] Hendrik G. Kruger[a*] and Bahareh Honarparvar[a*]

[a]Catalysis and Peptide Research Unit, School of Health Sciences, University of KwaZulu-Natal, Durban 4001, South Africa.

[b]School of Chemistry and Physics, University of KwaZulu-Natal, 4001 Durban, South Africa.

[c]Center for Tuberculosis Research, Division of Infectious Diseases, School of Medicine, Johns Hopkins University, Baltimore, MD 21205, USA.

[d]GlaxoSmithKline PLC, 1250 S. Collegeville Rd., Collegeville, PA, 19426, USA.

[e]Department of Chemistry and Biochemistry, University of California San Diego, 9500 Gilman Drive, La Jolla, CA 92093, USA.

***Corresponding authors:** Honarparvar@ukzn.ac.za (Dr Bahareh Honarparvar), (Prof. Hendrik G. Kruger) kruger@ukzn.ac.za, Telephone: + 27 31 2601845, Fax: +27 31 2603091, Catalysis and Peptide Research Unit, School of Health Sciences, University of KwaZulu-Natal, Durban 4041, South Africa.

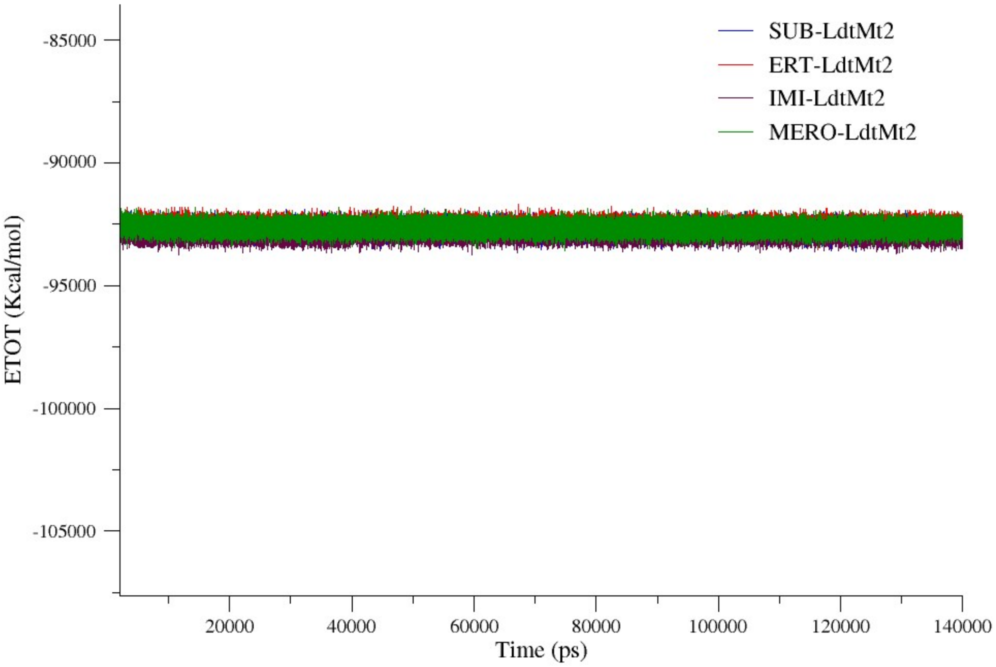

Figure S1. The total system energy (E_{tot}) of the SUB-Ldt_{Mt2}, ERT-LdtMt2, IMI-Ldt_{Mt2} and MERO-Ldt_{Mt2} during the 140 ns MD simulation is presented.

Table S1. The protonation states of the enzyme residues. The catalytic residues of Ldt$_{Mt2}$ are presented in bold.

Residues	**Pka**
HIS 1	5.94
LEU 2	7.57
TYR 6	11.7
ASP 11	3.98
GLU 13	2.75
GLU 19	6.28
ARG 24	13.16
ASP 26	3.13
GLU 27	3.90
ASP 31	3.37
ARG 32	11.93
GLU 36	5.18
LYS 37	10.42
LYS 40	10.33
GLU 48	4.60
TYR 52	9.98
ARG 57	12.32
GLU 58	3.74
ARG 60	14.65
ARG 62	10.25
GLU 64	4.65
HIS 65	6.47
LYS 68	10.55
ASP 74	4.03
TYR 80	10.19
ASP 83	2.71
GLU 86	4.80
GLU 91	4.79
ASP 92	3.38
HIS 97	7.46
ASP 102	3.29
GLU 103	4.77
ASP 109	1.48
ASP 110	3.67
LYS 113	10.21
ARG 118	12.37

Residues	**Pka**
GLU 122	4.58
LYS 125	10.22
LYS 133	10.08
ASP 134	3.13
GLU 122	4.58
TYR 143	12.11
ARG 148	12.32
TYR 149	10.29
LYS 150	10.47
HIS 151	8.34
ASP 155	1.81
SER 156	SER 156
SER 157	SER 157
THR 158	THR 158
TYR 159	11.17
GLY 160	GLY 160
TYR 169	10.89
ARG 170	13.23
ASP 172	4.05
ASP 174	4.35
TYR 181	11.03
HIS 187	**4.4**
HIS 198	6.29
HIS 203	**5.02**
CYS 205	**11.61**
TYR 217	9.96
ASP 218	3.94
HIS 219	6.56
LYS 221	10.42
ARG 222	13.71
ASP 224	5.52
GLU 227	4.64
ASP 240	2.88
ASP 244	4.34
ASP 250	3.08
ARG 253	13.28
LYS 258	10.55

Table S2. The tip-tip distances of the β-hairpin flap in SUB-Ldt$_{Mt2}$ are presented.

Flap tips	Average distance (Å)	Max. value	Min. value
ASP134-SER165	18.36	25.17	12.7
ASP134-PRO166	16.73	25.49	9.25
ASP134-ASN167	13.24	20.67	9.04
SER135-SER165	14.16	20.93	8.87
SER135-PRO166	12.78	21.52	5.69
SER135-ASN167	**9.13**	**16.61**	**5.1**
THR136-SER165	13.98	20.28	9.8
THR136-PRO166	13.53	21.5	7.57
THR136-ASN167	**9.15**	**16.95**	**4.9**

Furthermore, the tip-tip distance analysis between THR136 (285)–ASN167 (316) residues reveals the highest peak value corresponded to ERT—Ldt$_{Mt2}$ complex with the lowest distance of 6.82 Å in a close conformation (**Figure S7**). For MERO—Ldt$_{Mt2}$ and IMI—Ldt$_{Mt2}$, the width of the frequency demonstrates the highest population in the close conformation is observed for MERO—Ldt$_{Mt2}$ than IMI-Ldt$_{Mt2}$.

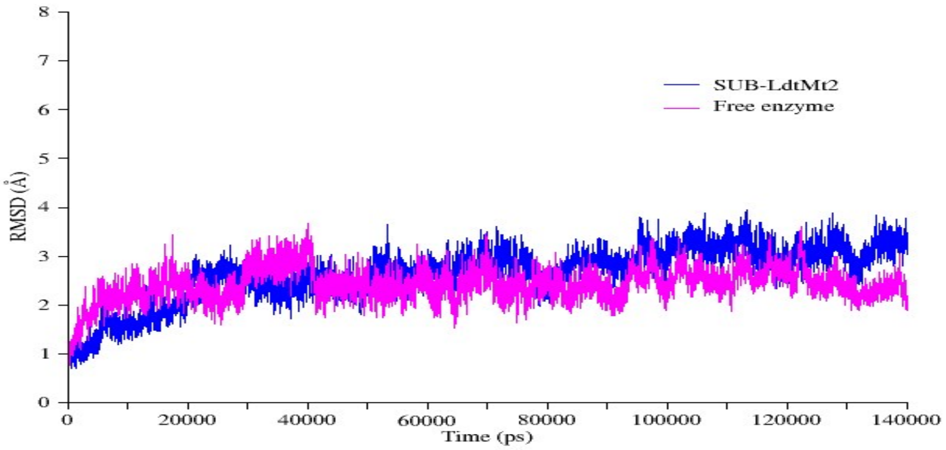

Figure S2. The RMSD of the backbone atoms relative to the corresponding to the free Ldt$_{Mt2}$ (pink), SUB-Ldt$_{Mt2}$ complex (blue), as the function of 140 ns MD simulation time.

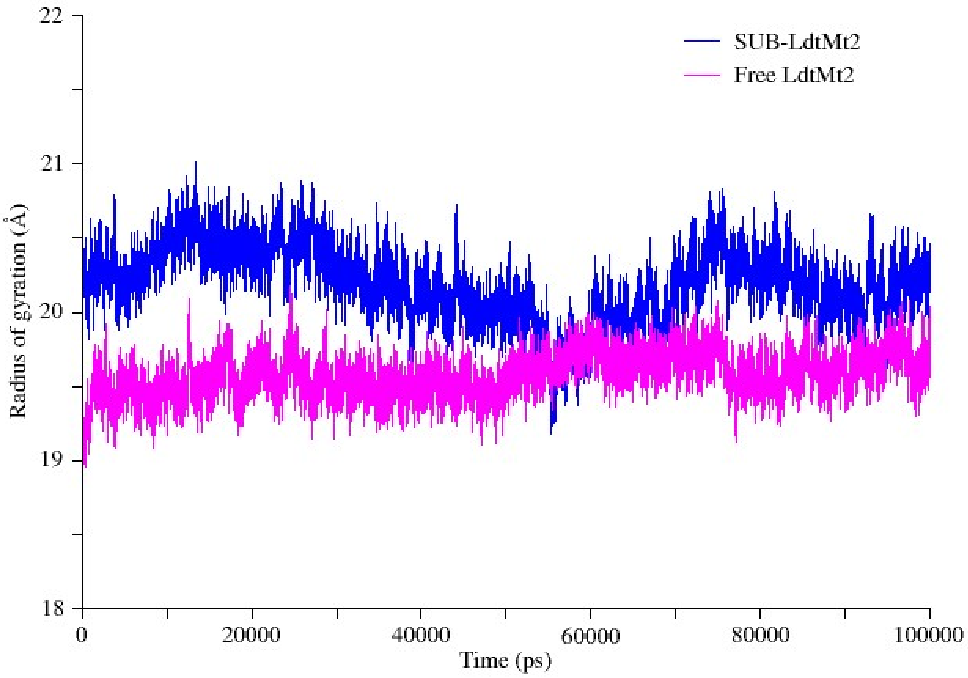

Figure S3. The plot of the radius of gyration (Rg) for the free Ldt_{Mt2} and SUB-Ldt_{Mt2} complex over the last 100 ns MD simulations.

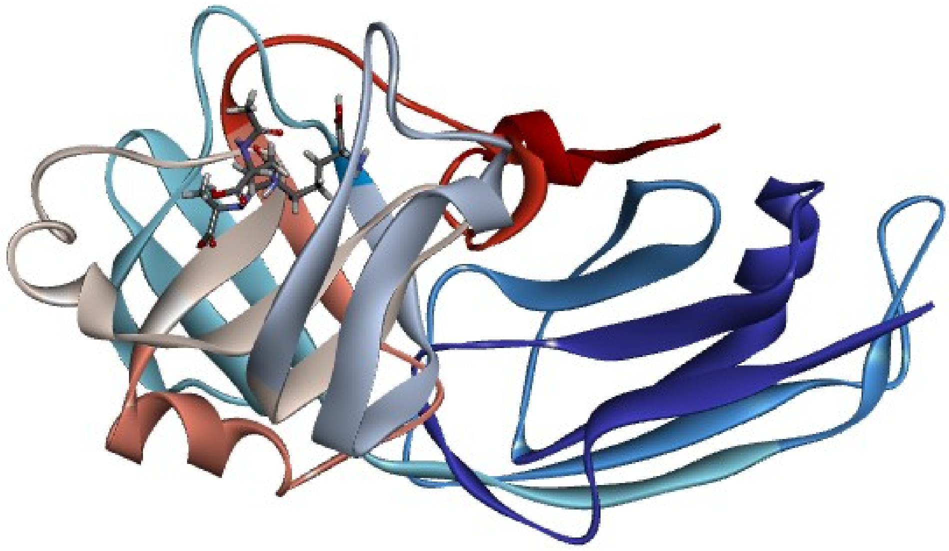

Figure S3-1. The per residue color scale based RMSF presentation of SUB-Ldt_{Mt2} complex.

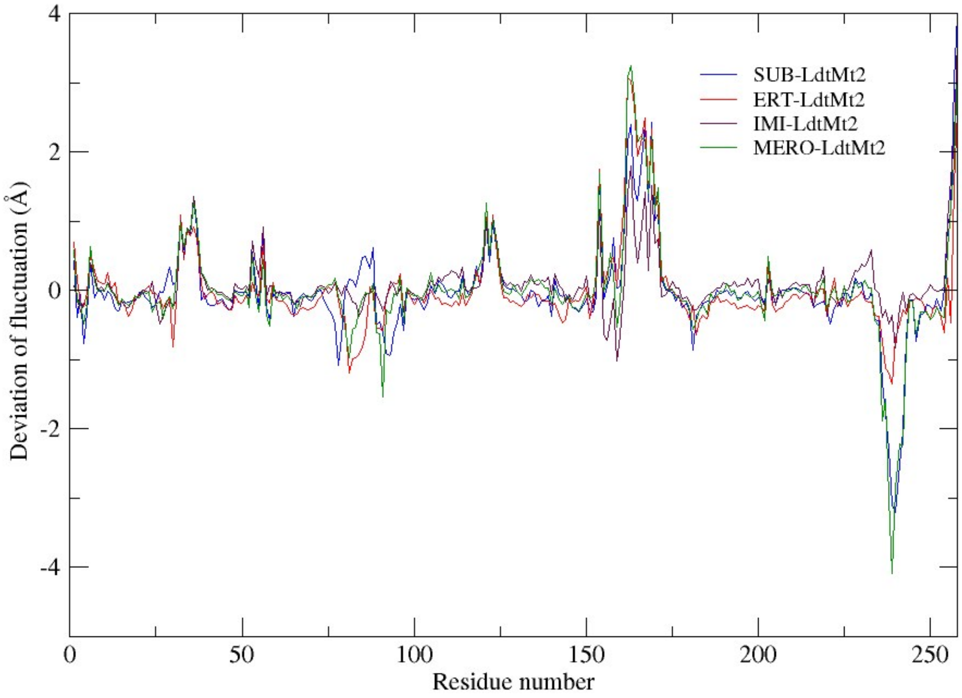

Figure S3-2. Fluctuation deviation metric of SUB-Ldt$_{Mt2}$, ERT-Ldt$_{Mt2}$, IMI-Ldt$_{Mt2}$ and MERO-Ldt$_{Mt2}$ over MD trajectories. The free Ldt$_{Mt2}$ was considered as reference to measure the fluctuation deviation.

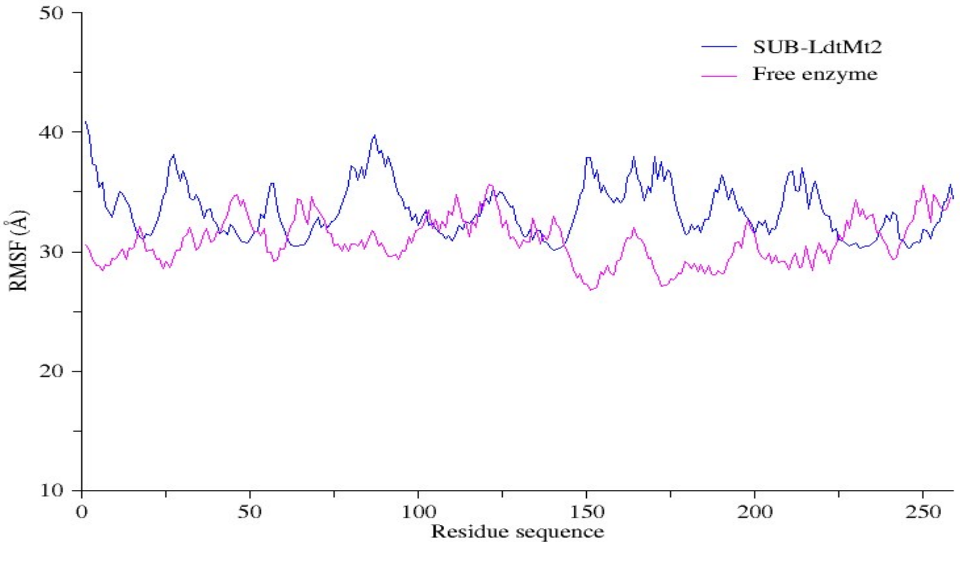

Figure S4. The per-residue RMSF of Cα atoms for the free Ldt$_{Mt2}$ (pink) and SUB-Ldt$_{Mt2}$ complex (blue) in terms of residue number.

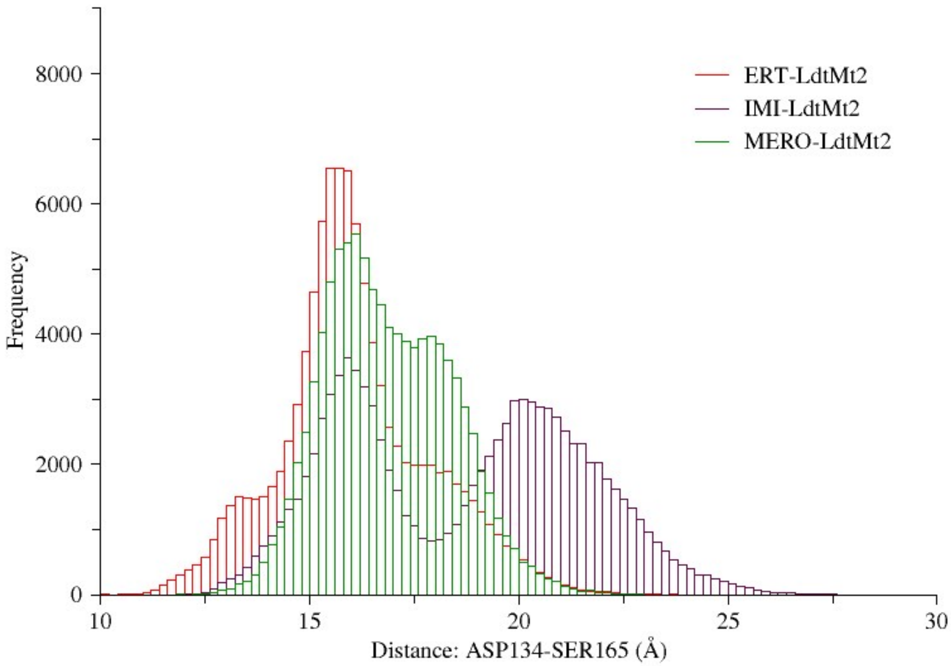
8000
6000
4000
2000
0
Frequency
10
15
20
25
30
Distance: ASP134-SER165 (Å)
ERT-LdtMt2
IMI-LdtMt2
MERO-LdtMt2

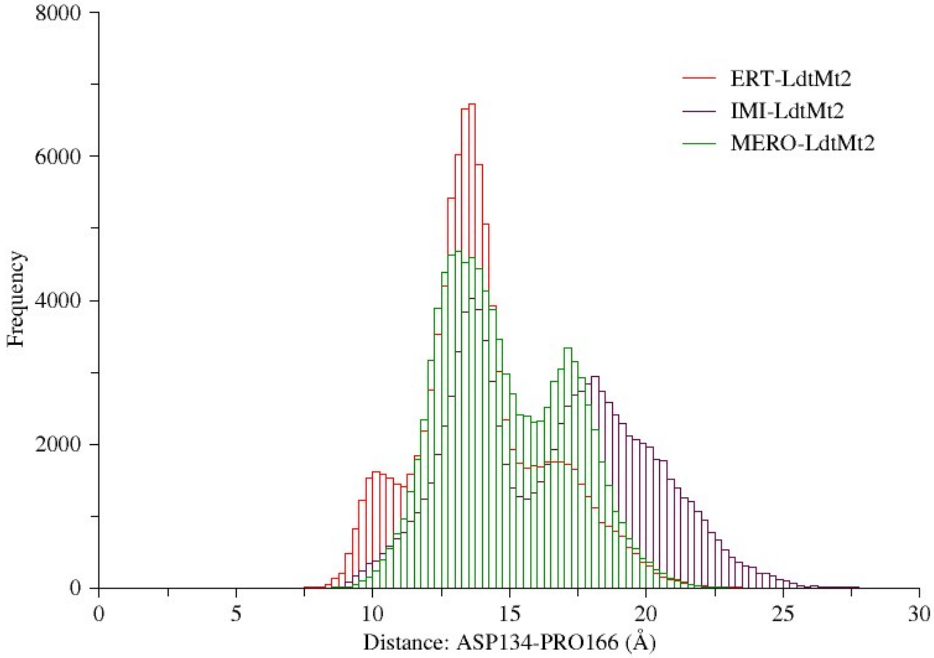
8000
6000
4000
2000
0
Frequency
0
5
10
15
20
25
30
Distance: ASP134-PRO166 (Å)
ERT-LdtMt2
IMI-LdtMt2
MERO-LdtMt2

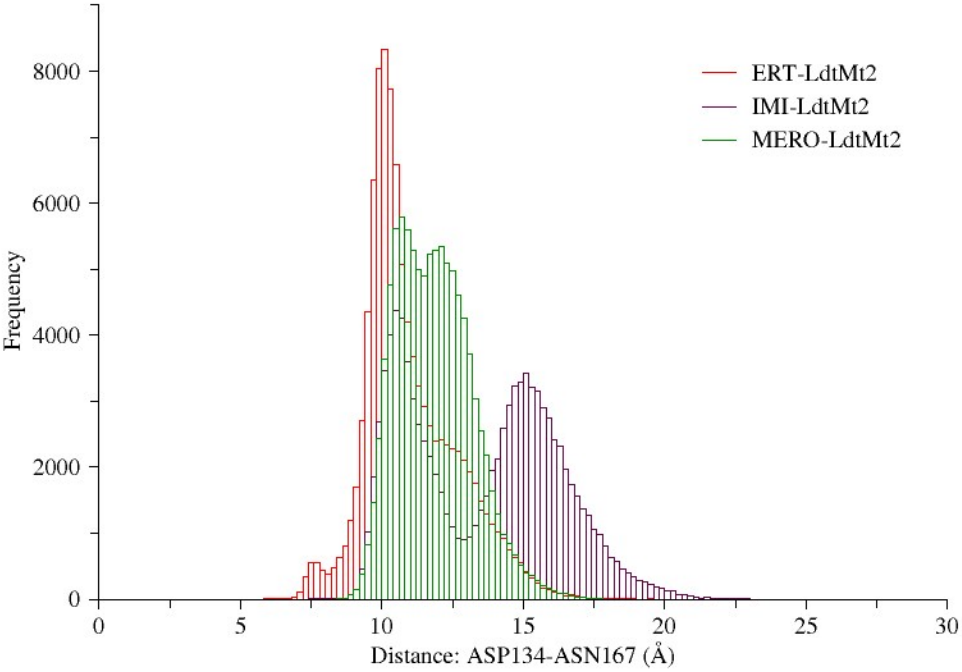
Frequency
0
2000
4000
6000
8000
0
5
10
15
20
25
30
Distance: ASP134-ASN167 (Å)
ERT-LdtMt2
IMI-LdtMt2
MERO-LdtMt2

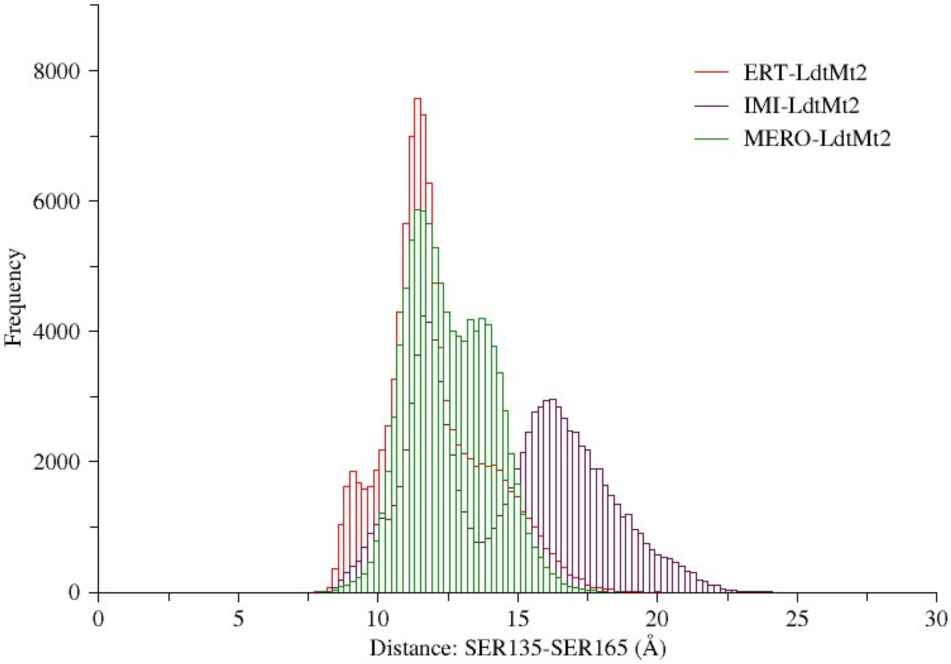
Frequency
0
2000
4000
6000
8000
0
5
10
15
20
25
30
Distance: SER135-SER165 (Å)
ERT-LdtMt2
IMI-LdtMt2
MERO-LdtMt2

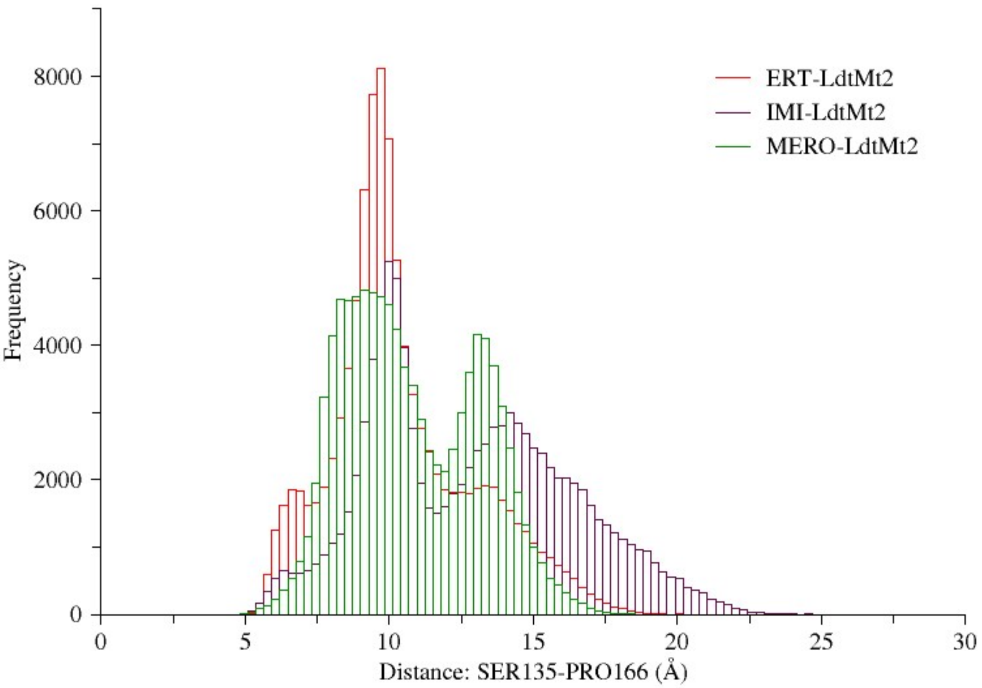
8000
6000
4000
2000
0
Frequency
0
5
10
15
20
25
30
Distance: SER135-PRO166 (Å)
ERT-LdtMt2
IMI-LdtMt2
MERO-LdtMt2

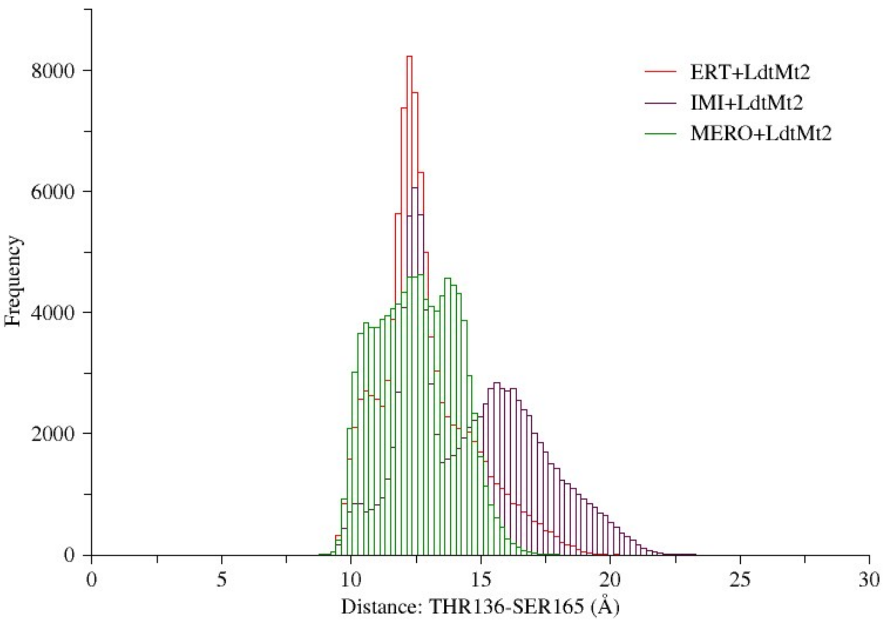
8000
6000
4000
2000
0
Frequency
0
5
10
15
20
25
30
Distance: THR136-SER165 (Å)
ERT+LdtMt2
IMI+LdtMt2
MERO+LdtMt2

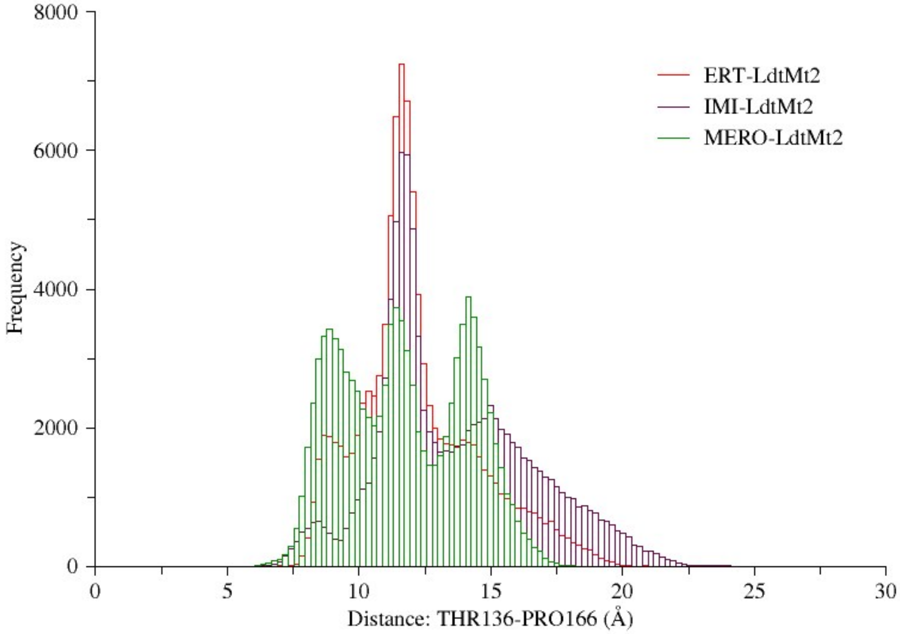

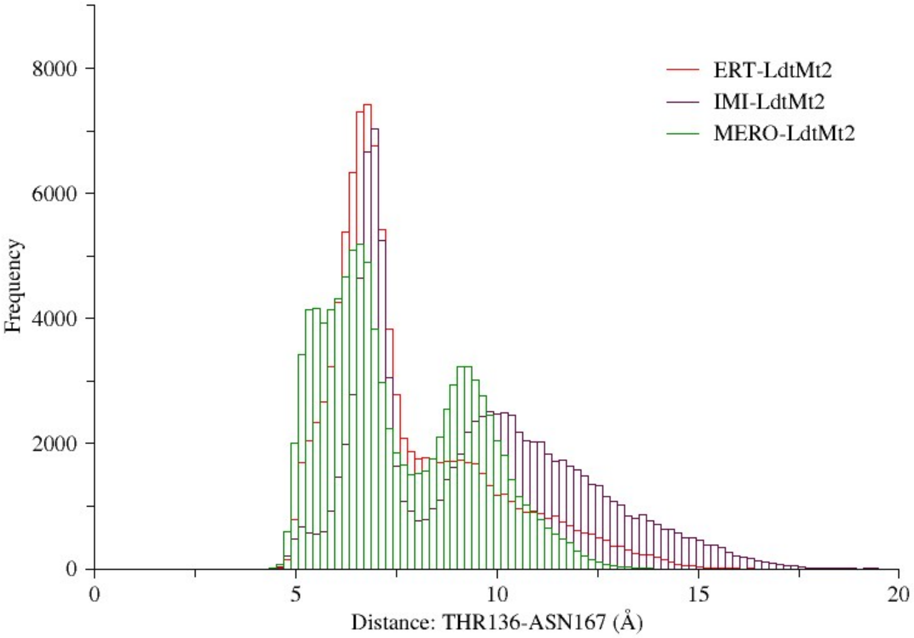

Figure S7. Histogram distribution of the tip-tip distances for ERT-Ldt$_{Mt2}$, IMI-Ldt$_{Mt2}$ and MERO-Ldt$_{Mt2}$ over the 100 ns MD trajectories: D1: ASP134−SER165, D2: ASP134−PRO166, D3: ASP134−ASN167, D4: SER135−SER165, D5: SER135−PRO166, D7: THR136−SER165, D8: THR136−PRO166, D9: THR136−ASN167.

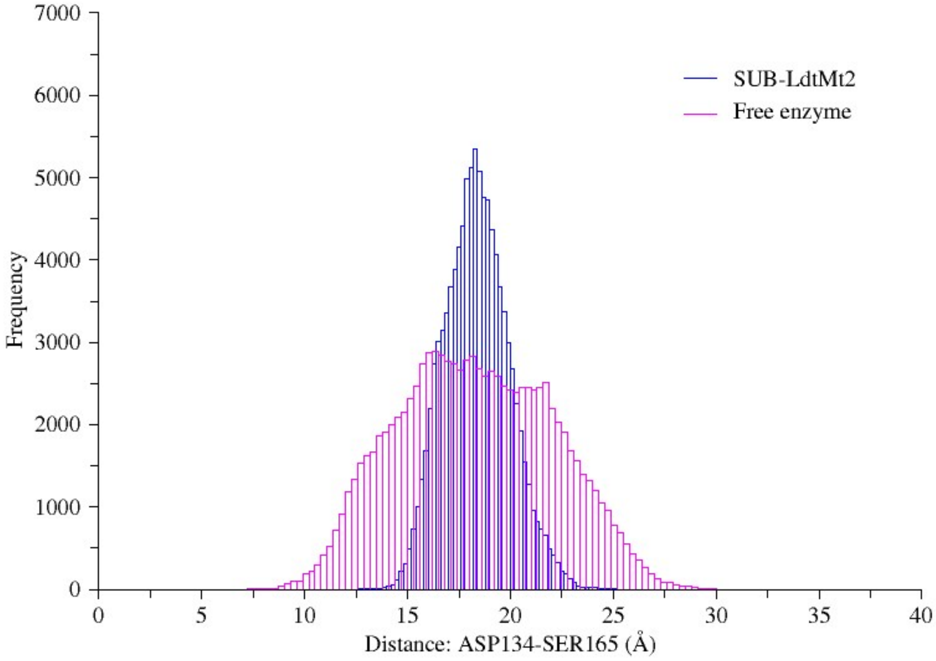
7000
6000
5000
4000
3000
2000
1000
0
Frequency
0
5
10
15
20
25
30
35
40
Distance: ASP134-SER165 (Å)
SUB-LdtMt2
Free enzyme

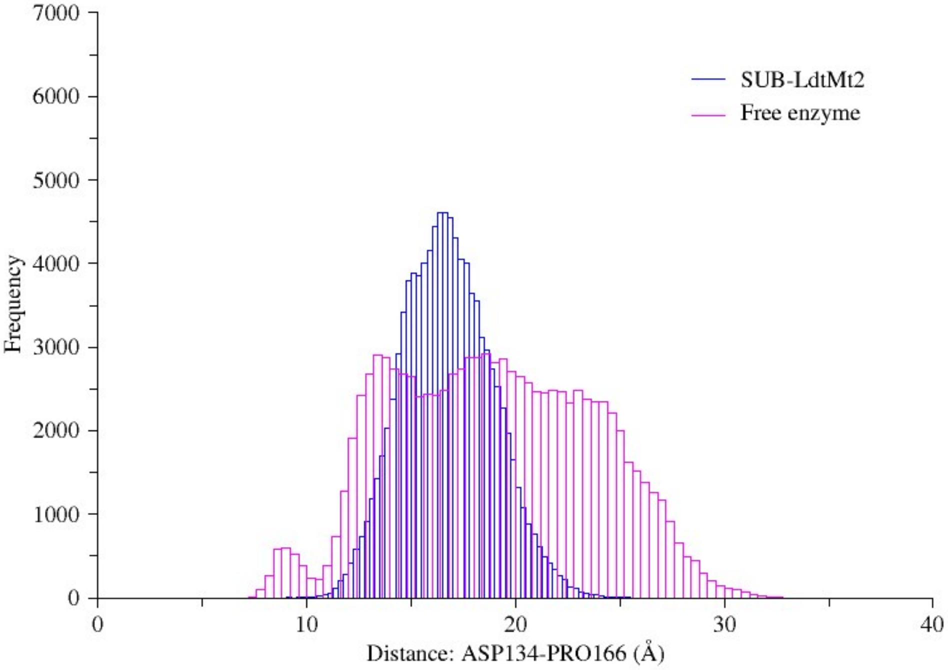
7000
6000
5000
4000
3000
2000
1000
0
Frequency
0
10
20
30
40
Distance: ASP134-PRO166 (Å)
SUB-LdtMt2
Free enzyme

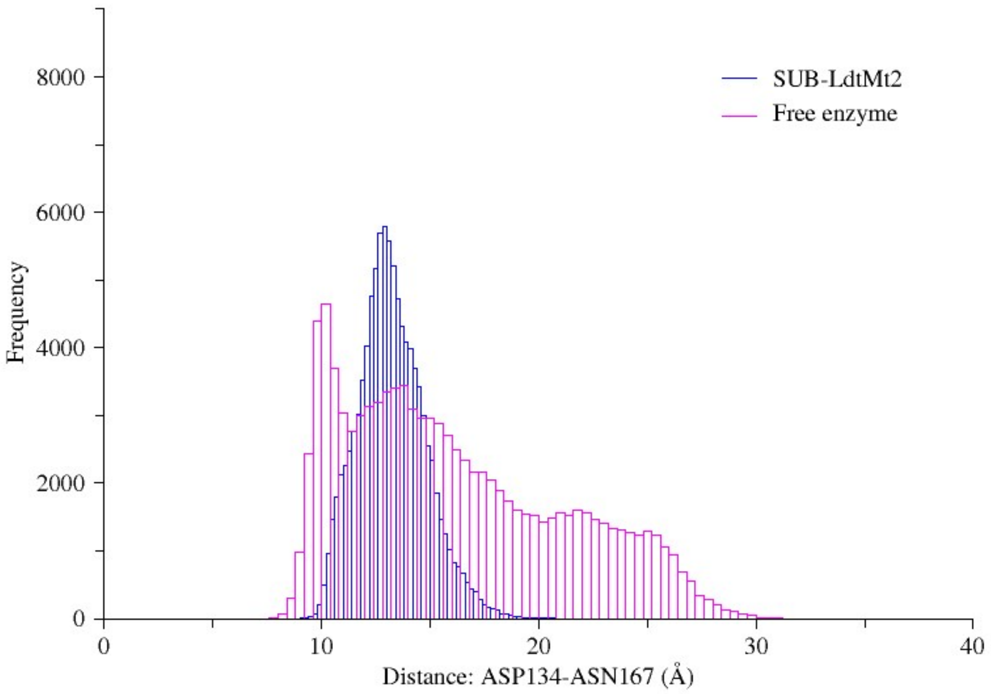
8000
6000
4000
2000
0
Frequency
0
10
20
30
40
Distance: ASP134-ASN167 (Å)
SUB-LdtMt2
Free enzyme

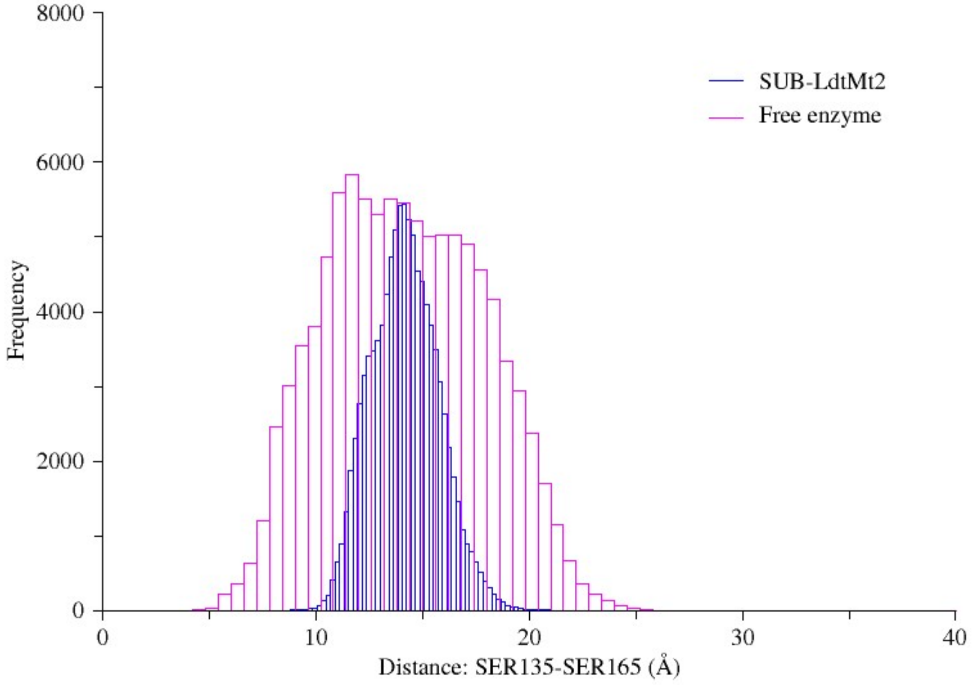
8000
6000
4000
2000
0
Frequency
0
10
20
30
40
Distance: SER135-SER165 (Å)
SUB-LdtMt2
Free enzyme

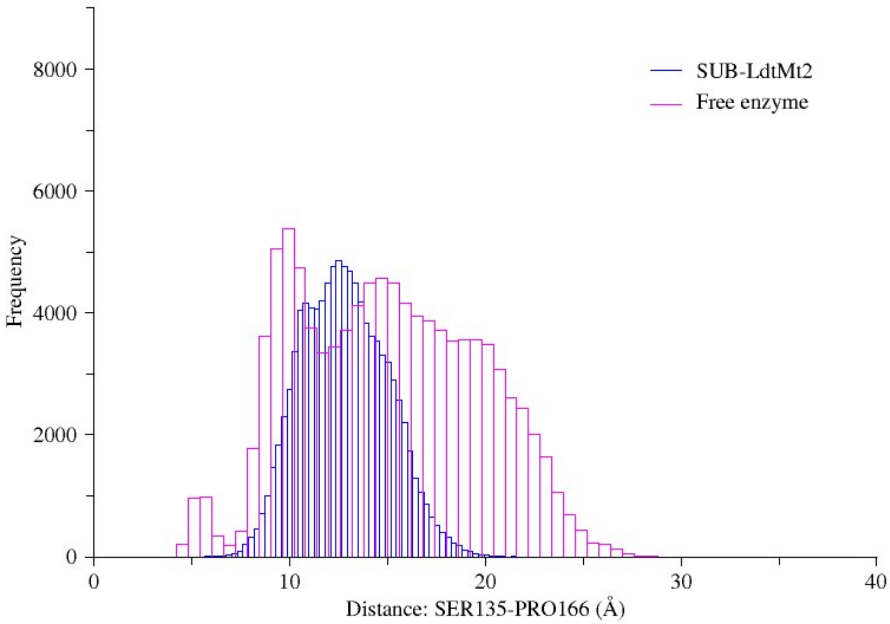
8000
6000
4000
2000
0
Frequency
0
10
20
30
40
Distance: SER135-PRO166 (Å)
SUB-LdtMt2
Free enzyme

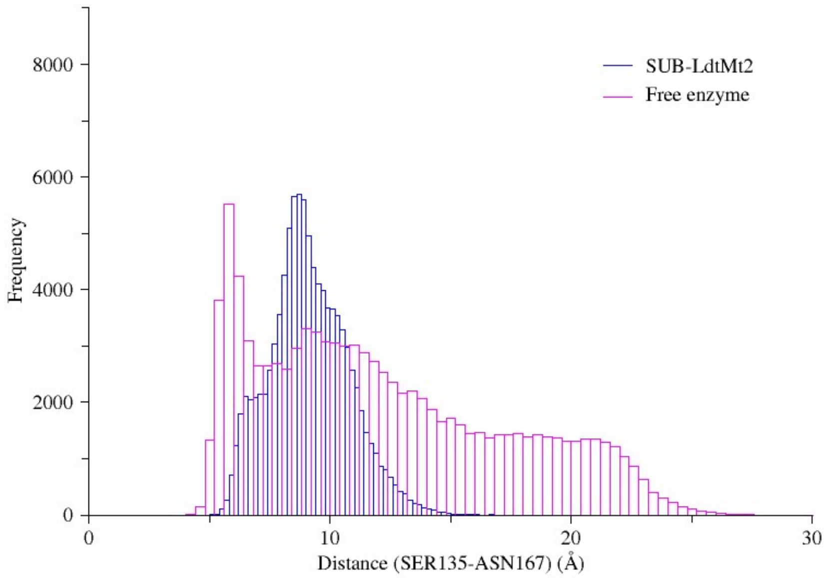
8000
6000
4000
2000
0
Frequency
0
10
20
30
Distance (SER135-ASN167) (Å)
SUB-LdtMt2
Free enzyme

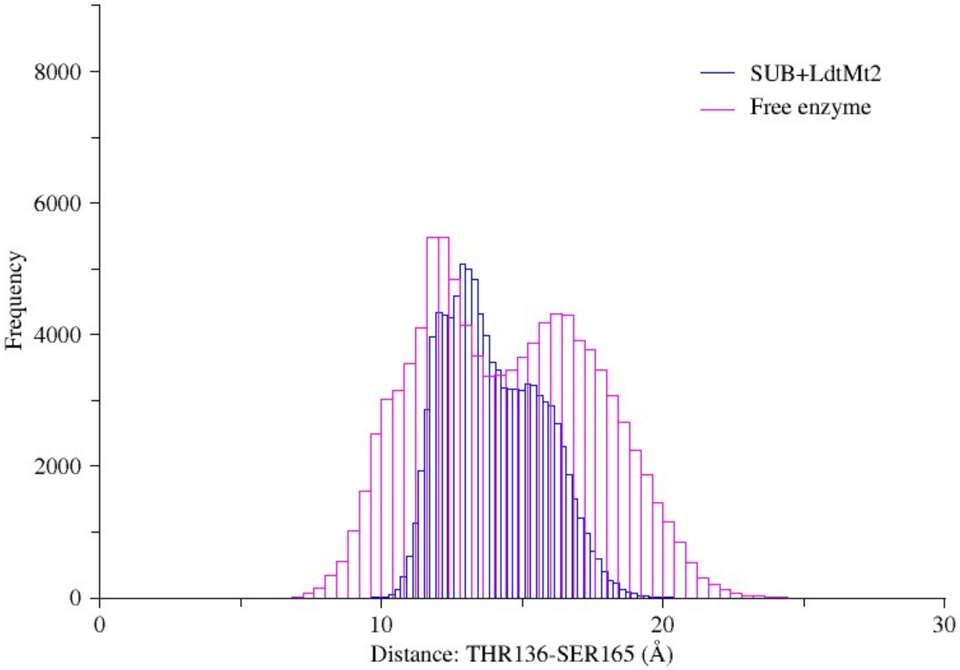

Figure S8. Histogram distribution of the tip-tip distances for SUB-Ldt$_{Mt2}$, free Ldt$_{Mt2}$ over the 100 ns MD trajectories: ASP134−SER165, ASP134−PRO166, ASP134−ASN167, SER135−SER165, SER135−PRO166, SER135−ASN167, THR136−SER165, THR136−PRO166, THR136−ASN167.

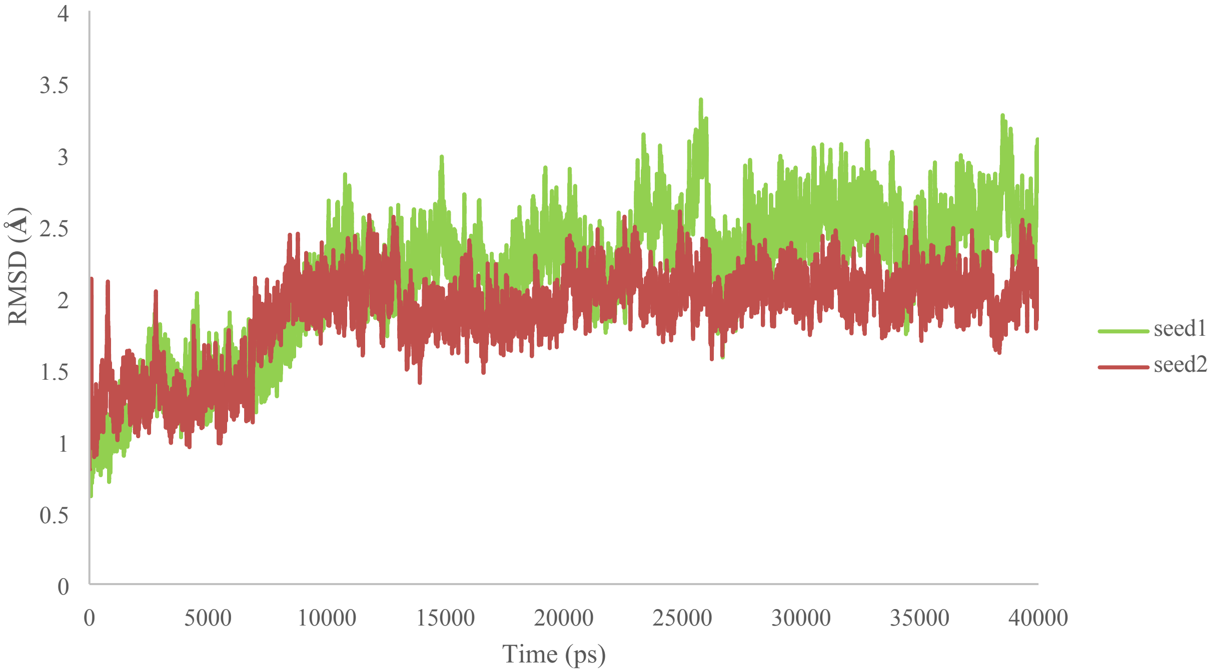

Figure S9. RMSD plot of backbone atoms of $\mathrm{Ldt}_{\mathrm{Mt2}}$ over two 40 ns MD trajectories.